Photoneutron cross section for ^{4}He

B. L. Berman, D. D. Faul, P. Meyer, and D. L. Olson
Lawrence Livermore Laboratory, University of California, Livermore, California 94550
(Received 15 January 1980)

The photoneutron cross section for ^{4}He has been measured from threshold up to 47 MeV using monoenergetic photons and a high-pressure gas sample. The results agree with earlier monoenergetic-photon and certain photoneutron time-of-flight (liquid-sample) results at the lower energies, and consequently disagree with the results of other measurements at these energies. At the higher energies, however, the present results are essentially in agreement with all previous results.

[NUCLEAR REACTIONS ^{4}He(γ,n); measured $\sigma(E_\gamma)$, 21 to 47 MeV, with monoenergetic photons, 4π neutron detector, high-pressure gas sample; four-nucleon system; isospin mixing; charge asymmetry.]

I. INTRODUCTION

The ratio of the photoproton and photoneutron cross sections for ^{4}He is a sensitive indicator of the degree of isospin mixing which is present in the simple ^{4}He nucleus and thus provides one with a quantitative test of the degree to which the charge symmetry of the nuclear force might be broken.[1,2] However, although there has been more or less general agreement for the ^{4}He(γ,p)^{3}H cross section,[3,4] there are large discrepancies between the published experimental results for the ^{4}He(γ,n)^{3}He cross section, particularly in the energy region below about 30 MeV [the (γ,n) threshold is 20.58 MeV (Ref. 5)].

Numerous experiments have been performed in the attempt to establish a definitive ^{4}He(γ,n) cross section (see Ref. 6 for a recent discussion of these measurements). Indeed, no fewer than eleven measurements have been reported: three total photoneutron measurements, two using bremsstrahlung,[7,8] and one using monoenergetic photons[9]; three photoneutron time-of-flight measurements (using bremsstrahlung), one at a single angle[10] and two at several angles[11,12]; four measurements of the recoil ^{3}He particles, three (using bremsstrahlung) with cloud chambers[13-15] and one (using virtual photons) with a magnetic spectrometer[16]; and one (inverse) ^{3}He neutron-capture measurement.[17] [The ratio measurement reported in Ref. 6 does not constitute an independent measurement of the absolute (γ,n) cross section.]

There is a serious controversy (discussed in Ref. 6) among these published results in the energy region between about 26 and 29 MeV, where the ^{4}He(γ,p) cross section is about 1.7 to 1.9 mb.[3,4] The (γ,n) cross-section results of Refs. 9 and 10 are "low" (~1.0 mb), while those of Refs. 12–14 are "high" (1.7 to 2.1 mb); those of Refs. 8, 11, and 15 are intermediate or open to some question (see Sec. III). In particular, since an important experimental question concerns the density of the helium sample used (see Refs. 6 and 18), it turns out to be important that the only measurement done with monoenergetic photons (Ref. 9) was done with a liquid helium sample. Therefore, it is of particular interest to perform a ^{4}He(γ,n) cross-section measurement with monoenergetic photons and a gas sample. Furthermore, since the controversy is concerned chiefly with the absolute magnitude of the cross section, the measurement must be done in such a way that careful attention is paid to the *systematic* uncertainties involved. We report here the results of such a measurement.

II. EXPERIMENT AND DATA REDUCTION

The measurement of the small ^{4}He(γ,n) cross section with a low-intensity monoenergetic-photon beam and a gas sample is inherently difficult owing to the low counting rates which result even with the use of an efficient neutron detector. The counting rates for the present measurement were made reasonable by the use of a high-pressure gas sample.

The general features, as well as many specific details, of the apparatus and procedures used for measuring photoneutron cross sections at Lawrence Livermore Laboratory (LLL) have appeared elsewhere in the recent literature.[19,20] The experimental layout is shown in Fig. 1. The source of radiation was the annihilation-photon beam produced by relativistic positrons from the LLL Electron-Positron Linear Accelerator passing through a 0.76-mm thick beryllium annihilation target. The photon beam was collimated by a series of three thick 9.5-mm diameter nickel collimators, and then allowed to pass through the high-pressure gas sample container located inside an efficient paraffin-and-BF_3-tube neutron detec-

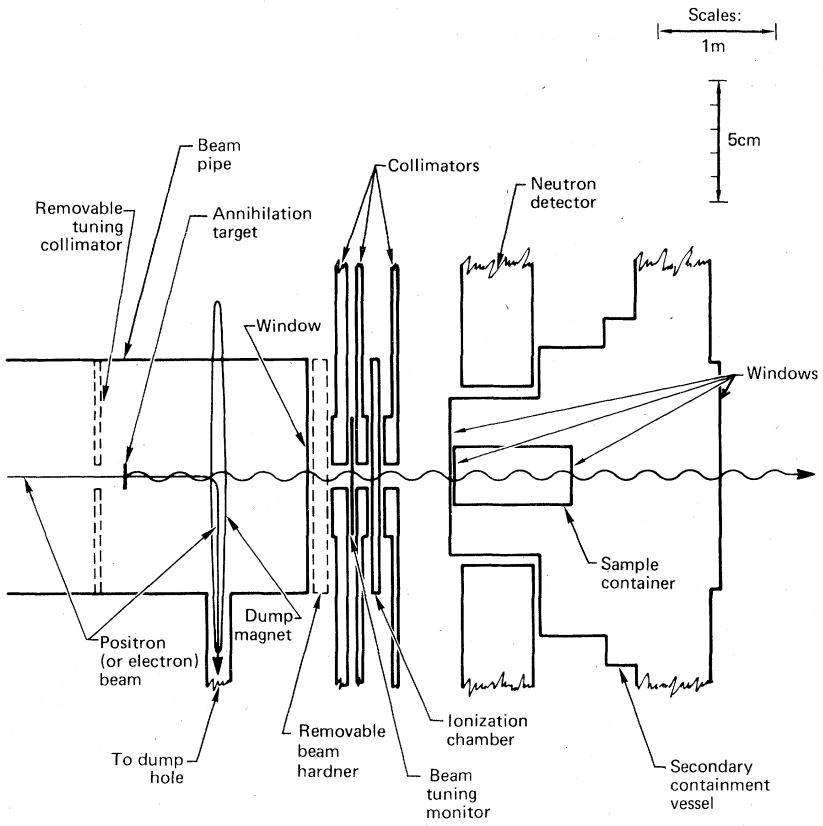

FIG. 1. Schematic diagram of the experimental layout for the present measurements with gas samples. Note the different horizontal and vertical scales. Shielding walls have been omitted for clarity.

tor. The photon beam flux was measured by a cylindrical xenon-filled thin-walled ionization chamber, which was calibrated against a large NaI photon spectrometer. The sample containers were stainless steel cylindrical tubes 1 m long and 2.54 cm inside diameter with welded end caps whose window thickness was 0.76 mm. A sample container was mounted inside the secondary containment vessel, a large evacuated stainless steel tank with 0.51-mm thick windows, capable of holding all the sample gas at less than atmospheric pressure. This secondary containment vessel in turn was moved into place inside the neutron detector (and its associated shielding). The alignment was check *in situ* with the aid of x-ray photographs made with the primary electron beam from the Linac. The 5.55-mole helium gas sample was contained at a pressure of 30.61 MPa (about 300 atm).

Background measurements with no annihilation target in place were made before and after each data run, and background measurements during a delayed gate were made simultaneously with each data run. Beam-off background measurements also were performed, and the drifts of both the ionization chamber and neutron detector were checked at frequent intervals with remotely controlled standard ^{60}Co and Am-Be radioactive sources. No rapid drifts, erratic behavior, or unusual effects of any other kind were encountered during the course of the experiment. Neutron-yield measurements for all samples were made with electrons, as well as with positrons, incident upon the annihilation target. Neutron-yield measurements also were made with an empty sample container, using oxygen, both in the form of gas and in the form of water, and with deuterium gas.

The data-analysis procedures for this experiment were largely the same as have been developed and used for many other photoneutron measurements at Lawrence Livermore Laboratory.[20] The cross section σ is obtained from the expression

$$\sigma = \frac{N}{Q}\frac{Q}{A}\,\mathrm{SAF}\,G\,\frac{1}{\epsilon},$$

where N/Q is the net number of neutrons per photon-flux monitor unit; Q/A is the number of such units per annihilation photon; SAF (the solid-angle factor) is the constant (for a given nuclear sample) which contains (i) the ratio of the solid angles sub-

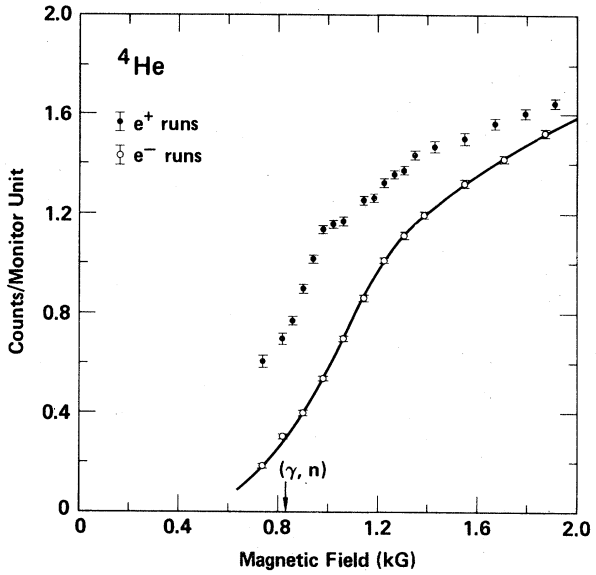

FIG. 2. Raw single-photoneutron yield data for ^{4}He, as a function of the magnetic field of the energy-analyzing magnet (1 kG corresponds to 24.8 MeV). The upper points (filled circles) are for incident positrons and the lower points (open circles) for electrons. The curve, which was fitted to the electron-yield data, was used for subtraction of the photoneutron yield resulting from positron bremsstrahlung. The ^{4}He(γ,n) threshold is indicated by the arrow.

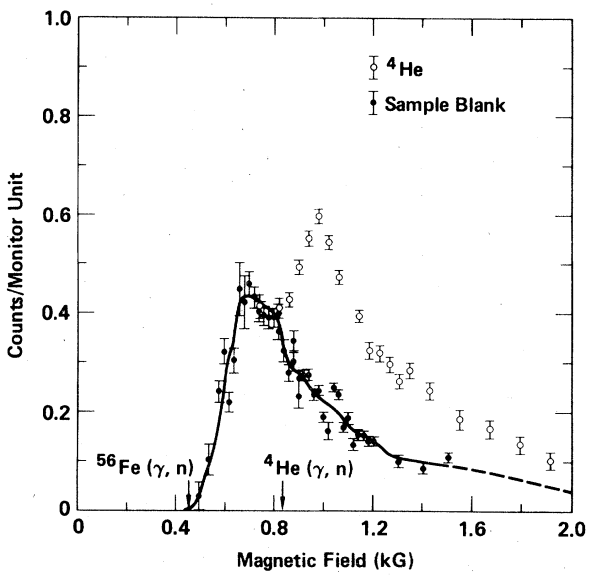

FIG. 3. Single-photoneutron yield data for ^{4}He (upper points, open circles) and for sample-blank runs (lower points, filled circles) after subtraction of the bremsstrahlung yields (1 kG corresponds to 24.8 MeV). The curve, which was fitted to the sample-blank data and extrapolated to higher energies (dashed curve), was used for the subtraction of the sample-blank background from the ^{4}He data to obtain the net ^{4}He yield. The principal source of the sample-blank background is the ^{56}Fe (γ,n) reaction on the steel windows: the sample-blank curve is seen to resemble the (γ,n) cross section for a nucleus like iron; the ^{56}Fe(γ,n) threshold also is indicated by an arrow.

tended at the annihilation target by the NaI spectrometer and by the neutron-producing sample and (ii) the effective number of sample atoms per unit area that are irradiated; $G = \mu T/(1 - e^{-\mu T})$, where μ is the photon attenuation coefficient of the sample per unit thickness and T is its thickness; and ϵ is the neutron detector efficiency. The net yield $N/Q = [(N/Q)^+ - k(N/Q)^-]$, where the superscripts $\pm$ indicate $e^\pm$ beams and k is the normalization constant[19] that accounts for their different ionization-chamber responses. The values for k at 13 different energies were remeasured and verified during the course of this experiment.

First, corrections to the N/Q data were made for pileup effects and for the various "no-beam" backgrounds and drifts. Figure 2 shows the raw single-photoneutron data for ^{4}He after these corrections were made, both for incident-positron and incident-electron runs, the latter multiplied by k. A smooth, monotonically increasing curve (also shown in Fig. 2) was fitted to the incident-electron neutron-yield data and used to subtract the neutron yields resulting from positron bremsstrahlung. This same procedure was followed for the sample-blank (empty-sample-container) runs, and the resulting (subtracted) annihilation-photon neutron yields, for both the sample-in and the sample-blank data, are shown in Fig. 3. Again, a smooth curve (also shown in Fig. 3) was fitted to the sample-blank data and used to subtract the sample-blank from the sample-in neutron yields. The same procedures were followed for the double-photoneutron data. In order to determine the normalization constant m by which the single-photoneutron sample-blank yield must be multiplied before subtraction from the single-photoneutron sample-in yield (to account for any small difference in background caused by imperfect alignment), the differences between the sample-in and sample-blank double-photoneutron yields for events below the ^{4}He$(\gamma,2n)$ threshold (28.3 MeV) were required to average to zero. This resulted in a value for m of 0.96, which has been included in the sample-blank data (and fitted curve) shown in Fig. 3. It should be emphasized here that the pileup rate for these measurements was exceedingly small (<0.5% even for the sample-in data), so that the double-neutron count rate, small as it was, resulted almost entirely from real $(\gamma,2n)$ reactions in the sample-container materials (experimental runs with no sample container present yielded no real double-neutron events at all). It was noted at this point that the net double-photo-

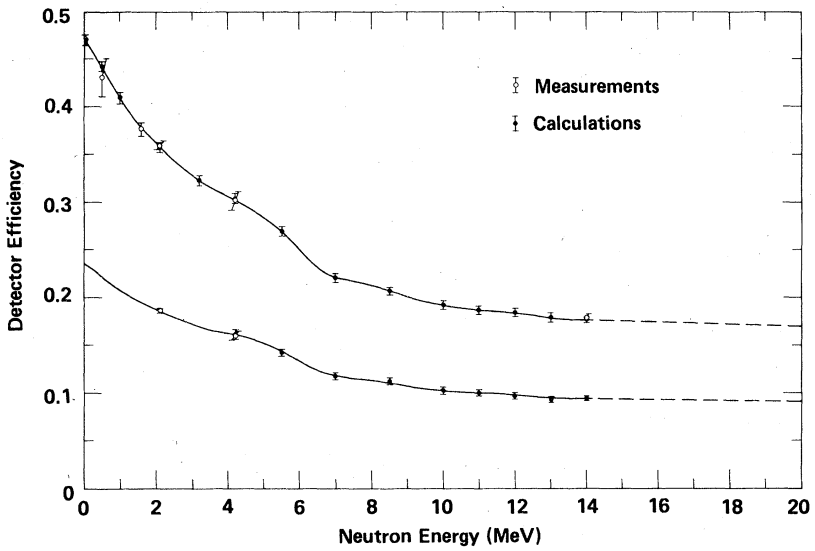

FIG. 4. Neutron detector efficiency, plotted as a function of neutron energy. The open circles represent experimental measurements; the filled circles represent Monte Carlo calculations. The curve fitted to the upper points is used as the efficiency for a sample located at the center of the 4π detector and from which neutrons are emitted isotropically; the lower curve [which is computed from the upper curve, multiplied by the factor $\langle f \rangle$ (see text)] is used as the efficiency for a sample distributed along the photon beam line through the detector as for the present gas-sample measurements (see Fig. 1), and from which neutrons are emitted with a $\sin^2\theta$ distribution with respect to the photon beam direction. Extrapolations to neutron energies above 14 MeV are shown as the dashed curves.

neutron yield for ^{4}He remained consistent with zero throughout the range of the experiment (up to 45 MeV), thus showing that $\sigma(\gamma, 2n)$ for ^{4}He remains negligible [compared with $\sigma(\gamma, n)$] up to 45 MeV. These procedures thus determined the net neutron yields per unit photon flux N/Q.

The absolute photon-flux calibration Q/A was rechecked and found to agree to within 2% with previous calibrations. It also was checked for both open (standard) and restricted (this measurement; see Fig. 1) collimation conditions and was found to scale, as it should, with collimator size. The other parameters necessary were the attenuation factor G of the photon beam in passing through the sample and windows, the functional dependence of the neutron-detector efficiency ϵ upon neutron energy E_n and (for the gas samples) upon position along the beam line, and the effective number of atoms in the samples (see below). The photon attenuation was small and easily accounted for; for the ^{4}He sample, $G = 1.06$ at 25 MeV and is only weakly energy dependent.

The neutron detector efficiency is plotted in Fig. 4 as a function of neutron energy. Even though the energy dependence of the detector efficiency at the center of the detector (the top curve in Fig. 4) is known well,[20] it was rechecked with Monte Carlo calculations with particular attention to the higher neutron energies (>4 MeV). These calculations extended up to 14 MeV, where a measurement had been made previously with a d-t neutron source; above this neutron energy (which corresponds to a photon energy E_γ of about 39 MeV for the photoneutron reaction on ^{4}He), a smooth extrapolation of the neutron-detector efficiency was used, shown by the dashed curves in Fig. 4. The falling off of the efficiency curve near 6 MeV results mainly from the ^{12}C(n, α) reaction, which acts as a sink of neutrons; knowledge of the energy dependence of this cross section[21] verifies the shape of the efficiency curve in this energy region. Finally, additional Monte Carlo calculations (not shown in Fig. 4) at six energies between 5.0 and 9.5 MeV (but with somewhat poorer statistics than the points shown in Fig. 4) corroborate both the magnitude and shape of the efficiency curve in this energy region.

The position dependence of the detector efficiency was measured (for neutrons having an average energy of 2.1 and 4.2 MeV) with standard ^{252}Cf and Pu-Be neutron sources. From these measurements, one obtains the factor $\langle f \rangle$ which converts ϵ into the effective efficiency for the distributed samples. [For $\sigma(\gamma, 2n)$, the factor $\langle f^2 \rangle$ (and not $\langle f \rangle^2$) converts ϵ^2 into the effective square of the efficiency needed.] Monte Carlo calculations of this function also were performed, which verified the source measurements and showed as well that there is no strong dependence of $\langle f \rangle$ or $\langle f^2 \rangle$ upon neutron energy. For the present case this is not important anyway, since it affects most strongly the $(\gamma, 2n)$ cross section and (through it) the multi-

plicity correction to the $(\gamma, 1n)$ cross section[20]; because the $^4\mathrm{He}(\gamma, 2n)$ cross section is very small (consistent with zero), the effect on the $^4\mathrm{He}(\gamma, n)$ cross section is negligible. In fact, above 4.2 MeV these functions are flat and equal to 0.533 and 0.422, and at 2.1 MeV they are equal to 0.519 and 0.417; therefore, below 4.2 MeV straight-line fits were used, which yield zero-energy values of 0.504 and 0.411 for $\langle f \rangle$ and $\langle f^2 \rangle$, respectively. The effective efficiency $\langle f \rangle \epsilon$ also is shown in Fig. 4 (the lower curve). Monte Carlo calculations of $\langle f \rangle \epsilon$ (modified by 1%; see below) are shown as the solid points in the lower part of Fig. 4, thus verifying that the curve drawn above 4.2 MeV is not significantly more uncertain than the upper curve of Fig. 4, which is verified in turn by the measurement at 14 MeV. Additional Monte Carlo calculations were performed in order to ascertain the effect of a $\sin^2\theta$ (rather than isotropic) distribution for the photoneutrons; the resulting correction factors, 1.01 for $\langle f \rangle$ and 1.02 for $\langle f^2 \rangle$, are included in the values given above and in the lower curve of Fig. 4. Still more Monte Carlo calculations showed that the presence of the ^{4}He gas in the sample container did not affect the detector efficiency (or $\langle f \rangle$). Finally, it should be noted that the energy dependence of $\langle f \rangle$, small as it is, is confined to neutron energies below 4.2 MeV; this corresponds to photon energies for the $^4\mathrm{He}(\gamma, n)$ reaction less than 26.2 MeV, since for this two-body breakup reaction, $E_n = 3(E_\gamma - 20.58\ \mathrm{MeV})/4$ is uniquely determined by the photon energy E_γ. [The three-body breakup threshold is 26.1 MeV, and the cross section $\sigma(\gamma, pn)$ for ^{4}He has been reported to be small, compared to $\sigma(\gamma, n)$, throughout the energy range studied here.[14,15]]

In order to determine the effective number of atoms in the ^{4}He sample intercepting the photon beam, three measurements using oxygen were made. The first was a new measurement of the absolute $^{16}\mathrm{O}(\gamma, n)$ cross section done in the usual way[19,20] using a water sample. The results of this measurement, reported in Ref. 22 and shown in Fig. 5, were found to agree very well with previous Livermore data[23] (except for a slight energy shift) and with more recent data from Giessen.[24] Next, the results of another water-sample oxygen measurement, which was performed under the same (restricted) collimation condition as was used with the ^{4}He sample, were normalized to these results; this determined the number of atoms in the beam (at the center of the neutron detector) for this collimation condition. Third, the results of a measurement using a high-pressure sample of oxygen gas, shown in Fig. 6, were normalized to the water-sample data; this determined the effective number of atoms in the oxygen gas sample

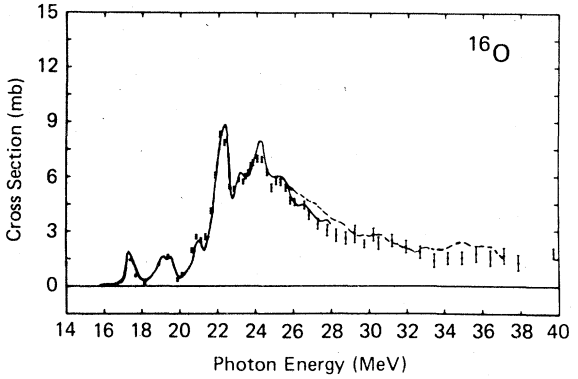

FIG. 5. Data points—recent Livermore measurement of the $^{16}\mathrm{O}(\gamma, n)$ cross section with a water sample (Ref. 22); solid curve—previous Livermore measurement (Ref. 23); dashed curve—Giessen measurement (Ref. 24). The Giessen data coincide with the Livermore data below 25 MeV.

intercepting the photon beam. Finally, the effective number of atoms in the ^{4}He sample was computed from the ratio of the number of moles of ^{4}He and ^{16}O in the two gas samples, determined gravimetrically to high accuracy (<0.3%). It should be emphasized that this procedure does not depend upon knowledge of the $^{16}\mathrm{O}(\gamma, n)$ cross section, although the agreement of these new results[22] with the previous data lends added confidence to the present results. It should be noted that because these oxygen data were taken over a significant range of photon (and neutron) energies, they serve to check that no strong energy-dependent systematic error is present.

Another (but less stringent) check on the overall absolute normalization is provided by the ^{2}H data, shown in Fig. 7. These data are seen to agree, within the (rather large) statistical experimental limits, with the Mainz total photo-absorption data[25] and the theoretical cross-section results of Breit.[26]

There are several possible sources of system-

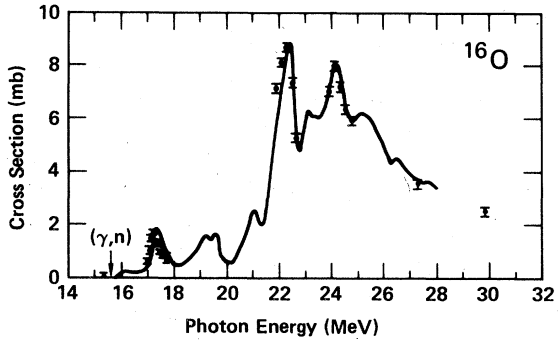

FIG. 6. Data points—present measurement of the $^{16}\mathrm{O}(\gamma, n)$ cross section with a gas sample; curve—previous Livermore measurement (Ref. 23).

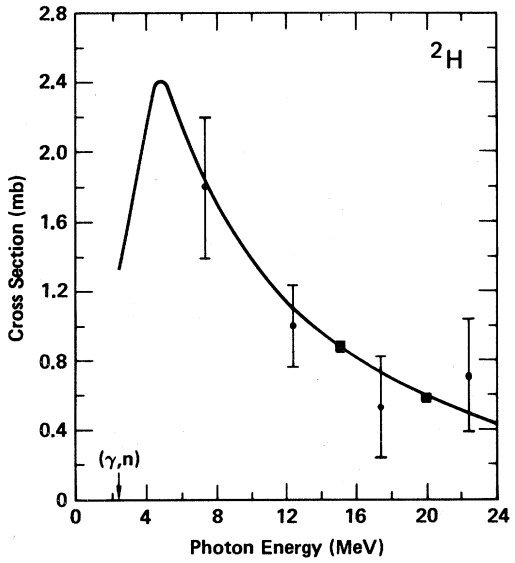

FIG. 7. Circles—present measurement of the ^{2}H(γ,n) cross section with a gas sample; squares—Mainz measurement (Ref. 25); curve—theoretical calculation (Ref. 26).

atic errors in the present experiment. The systematic uncertainty in the photon flux calibration is no greater than 5% at 22 MeV, but rises, more or less linearly with energy, to about 10% at 45 MeV. The uncertainty in the neutron-detector efficiency is less than 3% for neutrons of 2 MeV (corresponding to $E_\gamma \simeq 23$ MeV), but rises to about 5% for $E_n \simeq 14$ MeV and perhaps to $\gtrsim 8\%$ for $E_n \simeq 18$ MeV ($E_\gamma \simeq 45$ MeV). Thus, for the critical photon energy region from 26 to 29 MeV, the uncertainty in the detector efficiency is known not to exceed a few percent, and where it is not known well (>14 MeV), the statistical uncertainties of the data are much larger. The systematic uncertainty which arises from the bremsstrahlung-yield subtraction is roughly proportional to the incident-electron yield shown in Fig. 2, and is never more than 2% of that yield, which translates, for example, into about 10% of the cross section at 35 MeV. That which arises from the sample-blank subtraction is less than 5% at ~24 MeV, but in the high-energy region, where an extrapolated sample-blank yield had to be used (the dashed curve in Fig. 3), could very well be as much as 15% above 42 MeV. There is some cause for concern that the scatter in the sample-blank data points near 1 kG ($\gtrsim$25 MeV) has been ignored in the smoothing procedure (see Fig. 3); however, it happens that simply connecting adjacent sample-blank data points with straight-line segments (to reflect any possible structure in these data) would not affect the final results for ^{4}He significantly because the ^{4}He data points were obtained (by coincidence) at energies which lie

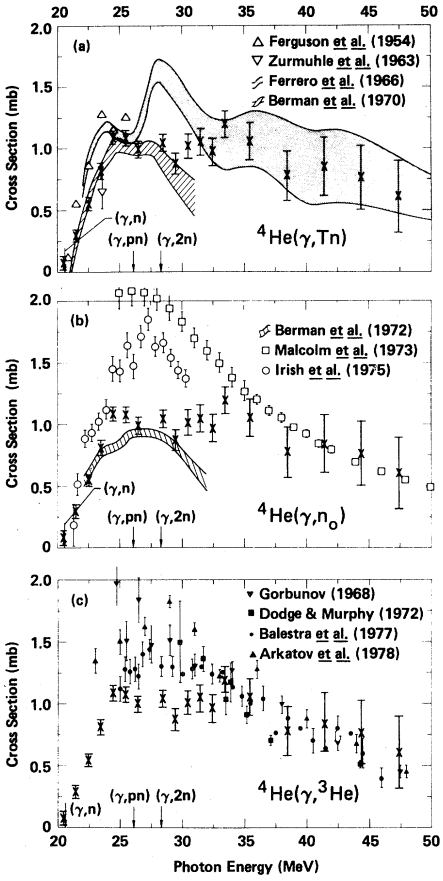

FIG. 8. Photoneutron cross section for ^{4}He. The present results are indicated as x's in all three parts of the figure. The error flags (except for those for the three highest-energy points; see text) represent statistical uncertainties only. Systematic uncertainties in the 25–28-MeV region could be as large as 15% (see text). (a) Present data compared with the photoneutron-yield results of Ref. 7 (Pennsylvania; open triangles), Ref. 8 (Torino; upper shaded band), Ref. 9 (Livermore; lower shaded band), and with the neutron-capture datum of Ref. 17 (Pennsylvania; open inverted triangle). (b) Present data compared with the photoneutron-time-of-flight data of Ref. 10 (Yale; shaded band), Ref. 11 (Toronto; open circles), and Ref. 12 (Saskatchewan; open squares). The 90° differential cross-section data of Ref. 10 have been converted to total cross sections using the angular-distribution coefficients of Ref. 11. The data of Ref. 11 were obtained with a liquid helium sample and later were renormalized to the results of a 98° measurement obtained with a gaseous sample (see text). (c) Present data compared with the cloud-chamber data of Ref. 13 (Moscow; filled inverted triangles), Ref. 14 (Kharkov; filled triangles), Ref. 15 (Torino; filled circles), and with the magnetic-spectrometer data of Ref. 16 (NBS; filled squares). The data of Ref. 16 were recalculated with the angular-distribution coefficients used in Ref. 6.

between the resulting structures in the sample-blank data. Still, the data points at 25.3 and 26.3 MeV (and perhaps the one at 28.3 MeV) should have larger systematic uncertainties attached to them, conceivably as large as 15%. It also might turn out, if the ^{56}Fe(γ,n) cross section were not typical of other nuclei in this mass region, that the extrapolation shown in Fig. 3 is in error; but this would affect only the three highest-energy ^{4}He points, which already have very large statistical uncertainties. All other systematic uncertainties are small by comparison with the above.

III. RESULTS AND DISCUSSION

The results of the present measurement of the ^{4}He(γ,n) cross section are shown in all three parts of Fig. 8. The estimated systematic uncertainty which results from the subtraction of the extrapolated sample-blank data (Fig. 3) are included in the error flags. The cross section is seen to rise sharply from threshold to a value of ~1.0 mb at 25 MeV, and then to remain roughly constant at a value near 1.1 mb for a wide energy interval up to about 35 MeV, before falling gradually to a value of about 0.7 mb at 45 MeV.

Figure 8(a) shows as well as the results of the photoneutron yield measurements,[7-9] along with the single neutron-capture datum.[17] The present data agree well with the results of Ref. 9 (Livermore) below 28 MeV and with those of Ref. 8 (Torino) from 24 to 26 MeV and above 32 MeV. The data of Refs. 7 and 17 (Pennsylvania) are slightly higher and lower, respectively, than the present results.

Figure 8(b) shows the results of the photoneutron time-of-flight measurements.[10-12] The 90° differential cross-section data of Ref. 10 (Yale) were converted to total cross sections with the use of the angular-distribution coefficients of Ref. 11. These results are in agreement with the present results below 30 MeV. The data of Ref. 11 (Toronto) need some discussion. These data were taken with a liquid sample at six angles, including 98°, and originally resulted in a maximum cross section of about 1 mb (see Ref. 27). Subsequently, data with a gas sample were taken (at 98° only, Ref. 18) and were found to result in a cross section a factor of 1.9 higher than the liquid-sample data. This discrepancy was thought to result from density changes in the liquid helium sample caused by beam heating.[18] The liquid-sample results therefore were multiplied by 1.9 and are presented as such in Ref. 11 and in Fig. 8(b). In view of the present results, it now appears that this normalization procedure perhaps should be reconsidered; a factor much smaller than 1.9 (and somewhat energy dependent) is needed to bring the results of Ref. 11 into agreement with the present results. The data of Ref. 12 (Saskatchewan) give the highest peak cross-section value of all twelve measurements (over 2 mb) and yet are in reasonable agreement with the present data above 35 MeV.

Figure 8(c) shows the results of the measurements where the ^{3}He particle was detected.[13-16] The cloud-chamber data of Refs. 13 (Moscow) and 14 (Kharkov) give peak cross-section values of about 1.7 mb between 26 and 29 MeV, and those of Ref. 15 (Torino) give a peak value of about 1.35 mb. However, there is good agreement between the results of all these measurements and the present results above about 33 MeV. The $(\gamma,{}^3\mathrm{He})$ cross sections from the electrodisintegration data of Ref. 16 (NBS) were recalculated with the angular-distribution coefficients used in Ref. 6 before being plotted in Fig. 8(c). (These values differ from those given in Ref. 16 by at most 12%.) These data do not extend down into the critical region below ~30 MeV, but are in reasonable agreement with the present results above that energy. However, the points at 37.1 and at 44.3 MeV appear to be appreciably lower than either the present or the consensus values at those energies; and it is at these energies, especially at 44 MeV, that the $\sigma(\gamma,{}^3\mathrm{H})$-to-$\sigma(\gamma,{}^3\mathrm{He})$ ratio results of Ref. 6 would require lower values for the ratio results of Ref. 16 [or higher $(\gamma,{}^3\mathrm{He})$ cross sections].

An attempt to reconcile all these disparate results cannot be made without casting considerable doubt upon several measurements; we can but try. The results of Ref. 9 probably fall off too rapidly above 28 MeV because the extrapolated neutron-detector efficiency used in Ref. 9 did not take account of the loss of neutrons via the ^{12}C(n,α) reaction (see Fig. 4). Those of Refs. 10 and 11 might do so because of an imperfect knowledge of the bremsstrahlung spectrum near its end point. Perhaps the normalization factor used in Ref. 11 was too large. No account was taken in Ref. 12 of the contamination of the low-energy part of the neutron spectrum by neutrons from the three- and four-body breakup of ^{4}He [a similar effect for a ^{4}He(γ,p) measurement performed at the same laboratory is readily apparent from a comparison of the (γ,p) and (γ,t) data in Ref. 28], and perhaps a problem exists as well with the bremsstrahlung spectrum used in Ref. 12 at energies far below the end points employed (50 to 110 MeV). And it is likely that cloud-chamber measurements of ^{3}He particles below about 3 MeV [corresponding to $E_\gamma = 33$ MeV for the ^{4}He$(\gamma,{}^3\mathrm{He})$ reaction] are so hard to make (when seen, they are short, single-track events near the beam) that the results of Refs. 13–15 are not trustworthy below ~33 MeV.[29] (Certainly it is hard to measure low-energy ^{3}He particles by other means, as can be seen from

Refs. 6 and 16.) If all these presumptions were true, however, then a consensus ^{4}He(γ,n) cross section could be synthesized from most of the data which would agree reasonably well (within the experimental limits) with the present results.

The integrated cross section $\sigma_{\rm int} = \int \sigma(E_\gamma) dE_\gamma$ measured in the present experiment [from the (γ,n) threshold up to $E_{\gamma\max} = 47.3$ MeV] is 23.1 ± 1.6 MeV mb. This uncertainty is statistical only, and should be increased to approximately twice this value when systematic uncertainties are taken into account. The present value for $\sigma_{\rm int}$ integrated up to 31.4 MeV is 9.0 MeV mb (with a smaller uncertainty, about 1 MeV mb), compared with the corresponding value of 7.9 MeV mb from Ref. 9. The present values for the first and second moments of the integrated cross section $\sigma_{-1} = \int \sigma(E_\gamma) E_\gamma^{-1} dE_\gamma$ and $\sigma_{-2} = \int \sigma(E_\gamma) E_\gamma^{-2} dE_\gamma$ are 0.71 mb and 0.023 mb MeV^{-1}, respectively, up to 47.3 MeV.

Comparing the present results (only) for the ^{4}He(γ,n) cross section with the (γ,p) cross section in the crucial 26–29 MeV energy region, we find a (γ,p)-to-(γ,n) cross-section ratio R between 1.6 and 1.9. This range of values for R implies a value for the isospin mixing [the ratio of amplitudes of the $T=0$ and $T=1$ components of the excited ^{4}He wave function (see Refs. 2 and 9)] of 0.14 ± 0.02. Since this amount of isospin mixing greatly exceeds that which can be expected from Coulomb effects alone,[9] it implies in turn a significant charge-asymmetric component of the nuclear force for the $T_z = 0$ member of the four-nucleon system near 27 MeV.

Calarco *et al.*[30] report the absolute ^{3}H(p,γ) cross-section measurement mentioned in Ref. 4, and compare the results of this measurement with the other absolute ^{4}He(γ,p) cross-section results in the literature. On the basis of the material presented both here and in Ref. 30, a comparative treatment of both the (γ,n) and (γ,p) cross sections will be given in Ref. 31; recommended values for these cross sections will be presented over the entire energy range from threshold to 50 MeV, and the wider implication of these values for the question of the charge symmetry of the nuclear force will be discussed.

ACKNOWLEDGMENTS

A preliminary version of this work was reported as Ref. 32. This work was performed at Lawrence Livermore Laboratory under the auspices of the U. S. Department of Energy under Contract No. W-7405-ENG-48.

[1] L. E. H. Trainor, Phys. Rev. 85, 962 (1952).
[2] F. C. Barker and A. K. Mann, Philos. Mag. 2, 5 (1957).
[3] W. E. Meyerhof and S. Fiarman, in *Proceedings of the International Conference on Photonuclear Reactions and Applications, Asilomar, 1973,* edited by B. L. Berman (Lawrence Livermore Laboratory, Livermore, 1973), p. 385.
[4] S. S. Hanna, in *Proceedings of the International Conference on Photonuclear Reactions and Applications Asilomar, 1973,* edited by B. L. Berman (Lawrence Livermore Laboratory, Livermore, 1973), p. 417.
[5] A. H. Wapstra and K. Bos, At. Data Nucl. Data Tables 19, 175 (1977).
[6] T. W. Phillips, B. L. Berman, D. D. Faul, J. R. Calarco, and J. R. Hall, Phys. Rev. C 19, 2091 (1979).
[7] G. A. Ferguson, J. Halpern, R. Nathans, and P. F. Yergin, Phys. Rev. 95, 776 (1954).
[8] F. Ferrero, C. Manfredotti, L. Pasqualini, G. Piragino, and P. G. Rama, Nuovo Cimento 45B, 273 (1966), reanalyzed in Ref. 15.
[9] B. L. Berman, S. C. Fultz, and M. A. Kelly, Phys. Rev. C 4, 723 (1971).
[10] B. L. Berman, F. W. K. Firk, and C.-P. Wu, Nucl. Phys. A179, 791 (1972).
[11] J. D. Irish, R. G. Johnson, B. L. Berman, B. J. Thomas, K. G. McNeill, and J. W. Jury, Can. J. Phys. 53, 802 (1975).
[12] C. K. Malcolm, D. V. Webb, Y. M. Shin, and D. M. Skopik, Phys. Lett. 47B, 433 (1973).
[13] A. N. Gorbunov, Phys. Lett. 27B, 436 (1968).
[14] Yu. M. Arkatov, P. I. Vatset, V. I. Voloshchuk, V. N. Gur'ev, and A. F. Khodyachikh, Ukr. Fiz. Zh. 23, 1818 (1978), which apparently supersedes several prior publications by Arkatov *et al.*
[15] F. Balestra, E. Bollini, L. Busso, R. Garfagnini, C. Guaraldo, G. Piragino, R. Scrimaglio, and A. Zanini, Nuovo Cimento 38A, 145 (1977), which supersedes the prior publications by Busso *et al.*
[16] W. R. Dodge and J. J. Murphy II, Phys. Rev. Lett. 28, 839 (1972).
[17] R. W. Zurmuhle, W. E. Stephens, and H. H. Staub, Phys. Rev. 132, 751 (1963).
[18] J. D. Irish, R. G. Johnson, B. L. Berman, B. J. Thomas, K. G. McNeill, and J. W. Jury, Phys. Rev. C 8, 1211 (1973); J. D. Irish, R. G. Johnson, K. G. McNeill, and J. W. Jury, *ibid.* 9, 2060 (1974).
[19] B. L. Berman and S. C. Fultz, Rev. Mod. Phys. 47, 713 (1975).
[20] J. G. Woodworth, K. G. McNeill, J. W. Jury, R. A. Alvarez, B. L. Berman, D. D. Faul, and P. Meyer, Lawrence Livermore Laboratory Report No. UCRL-77471 (1978) and Phys. Rev. C 19, 1667 (1979).
[21] E. A. Davis, T. W. Bonner, D. W. Worley, Jr., and R. Bass, Nucl. Phys. 48, 169 (1963).

[22]J. W. Jury, B. L. Berman, D. D. Faul, P. Meyer, and J. G. Woodworth, Phys. Rev. C 21, 503 (1980).
[23]R. L. Bramblett, J. T. Caldwell, R. R. Harvey, and S. C. Fultz, Phys. Rev. 133, B869 (1964); J. T. Caldwell, R. L. Bramblett, B. L. Berman, R. R. Harvey, and S. C. Fultz, Phys. Rev. Lett. 15, 976 (1965).
[24]U. Kneissel, E. A. Koop, G. Kuhl, K. H. Leister, and A. Weller, Nucl. Instum. Methods 127, 1 (1975).
[25]J. Ahrens, H. B. Eppler, H. Gimm, M. Kroning, P. Riehn, A. Zieger, and B. Ziegler, Phys. Lett. B52, 43 (1974).
[26]G. Breit, in *Proceedings of the International Conference on Photonuclear Reactions and Applications, Asilomar, 1973*, edited by B. L. Berman (Lawrence Livermore Laboratory, Livermore, 1973), p. 323.
[27]J. D. Irish, B. L. Berman, R. G. Johnson, B. J. Thomas, K. G. McNeill, and J. W. Jury, in *Proceedings of the International Conference on Few Particle Problems in Nuclear Physics*, edited by I. Slaus *et al.* (North-Holland, Amsterdam, 1973), p. 888.
[28]G. D. Wait, S. K. Kundu, Y. M. Shin, and W. F. Stubbins, Phys. Lett. 33B, 163 (1970).
[29]G. Piragino, Private communication (1980).
[30]J. R. Calarco, C. C. Chang, E. M. Diener, S. S. Hanna, E. Kuhlmann, and G. A. Fisher, Phys. Rev. C (to be published).
[31]J. R. Calarco and B. L. Berman, Phys. Rev. C (to be published).
[32]B. L. Berman, D. D. Faul, P. Meyer, and D. L. Olson, Bull. Am. Phys. Soc. 24, 648 (1979).